High-Rate Synthesis and Characterization of Brightly Luminescent Silicon Nanoparticles with Applications in Hybrid Materials for Photonics and Biophotonics

Mark T. Swihart*[a,b], Xuegeng Li[a,b], Yuanqing He[a,b], William Kirkey[a,c] Alexander N. Cartwright[a,c], Yudhisthira Sahoo[a,d], and Paras N. Prasad[a,d]
[a]Institute for Lasers, Photonics, and Biophotonics, and Departments of [b]Chemical Engineering, [c]Electrical Engineering, and [d]Chemistry
University at Buffalo (SUNY), Buffalo, NY USA 14260-4200

ABSTRACT

This presentation focuses on the synthesis and characterization of luminescent silicon nanoparticles that have potential as components of hybrid inorganic/organic materials for photonic and biophotonic applications. In our lab, silicon nanoparticles with bright visible photoluminescence are being prepared by a new combined vapor-phase and solution-phase process, using only inexpensive commodity chemicals. CO_2 laser-induced pyrolysis of silane is used to produce Si nanoparticles at high rates (20 to 200 mg/hour). Particles with an average diameter as small as 5 nm can be prepared directly by this method. Etching these particles with mixtures of hydrofluoric acid (HF) and nitric acid (HNO_3) reduces the size and passivates the surface of these particles such that they exhibit bright visible luminescence at room temperature. The wavelength of maximum photoluminescence (PL) intensity can be controlled from above 800 nm to below 500 nm by controlling the etching time and conditions. Particles with blue and green emission are prepared by rapid thermal oxidation of orange-emitting particles. These particles have exciting potential applications in optoelectronics, display technology, chemical sensing, biological imaging, and other areas. The availability of relatively large quantities of these particles is allowing us to begin to functionalize particles for these applications, as well as to study the optical, electronic, and surface chemical properties of them. All of these potential applications require inorganic/organic hybrid materials, in the sense that the nanoparticles must have their surfaces coated with organic molecules that mediate the interaction of the particles with the polymeric or biological host matrix. The particle synthesis methods, photoluminescence measurements on the particles, the stability of the photoluminescence properties with time, chemical quenching of photoluminescence, and functionalization of the particles for incorporation into different organic matrices or for specific interaction with small molecules or biomolecules are discussed in the context of applications to photonics and biophotonics.

1. INTRODUCTION

The possibility of constructing optoelectronic devices, full-color displays, and sensors based on silicon has generated tremendous interest in the preparation and characterization of light emitting silicon nanoparticles. Because the particles' luminescence properties are size-dependent, multiple colors can be produced using a single material. These particles also have exciting potential applications as fluorescent tags for biological imaging, as has been proposed for II-VI compound semiconductor nanoparticles[1-3]. They can be brighter and much more stable to photobleaching than the organic dyes used in these applications, and they also have much broader excitation spectra, so that emission at multiple wavelengths (from particles of different sizes) can be excited by a single source. There are established methods for preparation of luminescent porous silicon[4], and aerosol synthesis of macroscopic quantities of non-luminescent silicon nanoparticles has been known for over 20 years[5,6]. However, producing macroscopic quantities (i.e. more than a few milligrams) of luminescent silicon nanoparticles that are free from a substrate has proven to be quite challenging. Soon after the initial discovery of photoluminescence from porous silicon[7], Brus and co-workers published a series of papers[8-11] in which they described the preparation of silicon nanoparticles by high temperature decomposition of disilane. These studies were instrumental in building understanding of photoluminescence

* swihart@eng.buffalo.edu; phone 1 716 645-2911 x2205; fax 1 716-645-3822

Proceedings of SPIE Vol. 5222 Nanocrystals, and Organic and Hybrid Nanomaterials, edited by David L. Andrews, Zeno Gaburro, Alexander N. Cartwright, Charles Y. C. Lee, (SPIE, Bellingham, WA, 2003) · 0277-786X/03/$15.00

mechanisms in silicon nanostructures. However, in their particle synthesis experiments, they collected less than 10 mg of particles per 24 hour day of reactor operation[9]. Carlisle *et al.*[12] and other groups have prepared small quantities of luminescent silicon nanoparticles by laser vaporization controlled condensation (LVCC). Recently, Korgel and co-workers prepared brightly luminescent silicon nanoparticles in supercritical organic solvents at high temperature (500 °C) and pressure (345 bar)[13-15]. Again, they have produced beautiful and well-characterized particles, but in quite small quantities. In their first report[15], 0.2 ml per batch of 250-500 mM diphenylsilane was converted to silicon nanoparticles with a yield of 0.5% to 5%, which corresponds to 0.07 to 1.4 mg of Si nanoparticles per batch. Nayfeh and coworkers, as well as a number of other groups, have produced brightly luminescent silicon nanoparticles by dislodging them from luminescent porous silicon wafers prepared electrochemically[16-18], and this has also generated tremendous technological and scientific interest. However, this method also generates small quantities of silicon nanocrystals, and the emitting nanocrystals may be embedded in larger porous silicon particles.

The first solution phase synthesis of Si nanoparticles was presented by Heath[19]. More recently Kauzlarich and co-workers have demonstrated several procedures[20-23] for producing silicon nanoparticles with a variety of surface terminations at mild conditions in solution using reactive Zintl salts. They are able to produce larger quantities of particles than the methods described in the previous paragraph. In some cases, they have shown blue-UV photoluminescence from these particles, but appear not to have observed the orange to red PL characteristic of porous silicon and most other nanoparticle preparation methods, including that presented here. Solid phase reactions have also been used to produce larger quantities of silicon nanoparticles, but apparently with much lower PL efficiency than the particles measured in the previous paragraph. Lam *et al.*[24] produced silicon nanoparticles by the reaction of graphite with SiO_2 in a ball mill. A wide range of particle sizes were produced, but some PL was observed after ball milling for 7 to 10 days.

CO_2 laser pyrolysis of silane is an effective method of producing gram-scale quantities of silicon nanoparticles, as first shown more than 20 years ago[5,6]. It produces high-purity loosely agglomerated particles with controlled primary particle size and size distribution. Moreover, it is a continuous process that permits reasonable production rates. While several groups have synthesized silicon particles with this and similar methods, the resulting particles showed little or no visible photoluminescence[25-27]. An exception to this is the work of Huisken and coworkers[28-31], who use pulsed CO_2 laser pyrolysis of silane, which yields luminescent particles directly, but in very small quantities.

In order to show efficient visible photoluminescence (PL), it is believed that silicon nanoparticles must be smaller than 5 nm, and their surface must be 'properly passivated' such that there are no non-radiative recombination sites on it. The mechanism(s) of photoluminescence in silicon nanocrystals and the effect of surface passivation on light emission from them remain topics of active research and debate. The size of silicon nanoparticles can be reduced by etching them in mixtures of hydrofluoric acid (HF) and nitric acid (HNO_3)[32]. We have recently discovered that a controlled HF/HNO_3 etching process can induce bright, visible photoluminescence in silicon nanoparticles produced by laser pyrolysis of silane that do not show significant photoluminescence before etching. In this paper, we first present this two-step particle synthesis process – laser pyrolysis synthesis followed by acid etching – and the photoluminescence properties of the resulting particles. These photoluminescence properties appear to be very similar to those of both porous silicon and the aerosol-synthesized particles produced in much smaller quantities by the Brus and co-workers and Huisken and co-workers as described above. With this ability to produce macroscopic quantities of particles, we are able to then explore functionalization of the particles' surfaces and dispersion of the particles in a variety of solvents and host matrices.

2. EXPERIMENTAL SECTION

The silicon nanoparticles were synthesized by laser-induced heating of silane to temperatures where it dissociates, in the reactor shown schematically in Figure 1. A continuous CO_2 laser beam (Coherent, Model 42 laser emitting up to 60 Watts) was focused to a diameter of about 2 mm just above the central reactant inlet. This inlet was made from 1/8 inch tubing centered within 3/8 inch tubing through which sheath gas, without reactants, flowed.. Silane (electronic grade, Scott Gases) weakly absorbs the laser energy at a wavelength of 10.6 microns, and is thereby heated. Sulfur hexafluoride (SF_6) may be added to the precursor stream as a photosensitizer. SF_6 (technical grade, Aldrich) has a

large absorption cross-section at the laser wavelength and can therefore dramatically increase the temperature achieved for a given laser power. Helium (UHP, passed through an oxygen trap to remove residual O_2 and H_2O) and hydrogen (ultrapure carrier grade) flows confine the reactant and photosensitizer (SF_6) to a region near the axis of the reactor and prevent them from accumulating in the arms of the 6-way cross from which the reactor is constructed. Hydrogen also serves to increase the temperature at which particle nucleation occurs, and to decrease the particle growth rate, since it is a by-product of silane dissociation and particle formation. All gas flow rates to the reactor were controlled by mass flow controllers. The resulting particles were collected on cellulose nitrate membrane filters. The effluent was directed to a furnace where it was heated to 850 C° to decompose any residual silane. This method can produce silicon nanoparticles at 20 to 200 mg per hour in the present configuration. With a commercially available multi-kilowatt laser focused into a thin sheet, one could readily scale this up by two orders of magnitude.

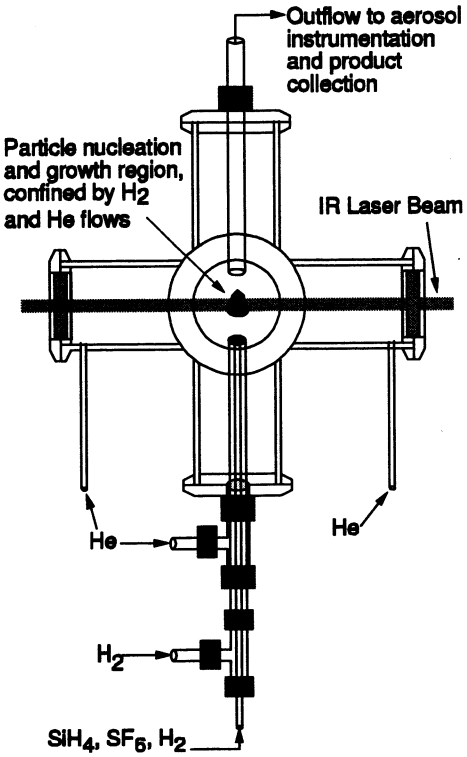

Figure 1: Schematic of laser-driven aerosol reactor

The powders obtained as described above were dispersed in methanol using mild sonication, then etched with solutions of 0.5 to 20% HF and 10% to 40% HNO_3 in water to reduce the particle size and passivate the particle surface. Acid solutions were prepared from 49-51 wt% HF, 68-70% HNO_3, and DI water in the necessary proportions. After etching, the particles were collected on polyvinylidene fluoride (PVDF) membrane filters (Millipore) and washed with DI water and methanol. Depending on etching conditions and initial particle size, 10% to 50% of the original particle mass is recovered after this process.

The silicon nanoparticles were characterized by transmission electron microscopy (TEM) and specific surface area measurements (Brunauer-Emmett-Teller method) prior to etching and by TEM after etching. Photoluminescence spectra (fluorescence spectra) were recorded with a Perkin-Elmer LS 50 fluorescence spectrometer with a 351 nm bandpass filter used to suppress any scattered light from the source. The excitation wavelength was set to 355 nm and the emission cutoff filter was set to 430 nm for most of the PL measurements shown here. For emission measurements on blue-emitting particles, the emission cutoff filter was set to 390 nm.

3. RESULTS AND DISCUSSION

3.1 Initial non-luminescent nanoparticles

TEM imaging shows that the as-synthesized powder in this case consists of nanocrystals with an average diameter near 5nm. While many particles are clearly visible in the TEM images, the image quality is not high enough to produce meaningful measurements of particle size distribution by particle counting. Nitrogen physisorption (the BET method, using Micromeretics model 2010 ASAP physisorption apparatus) was used to measure the specific surface area of particles. The highest measured surface area for these particles was 500 m^2/g. For spherical particles with the same density as bulk silicon, this is equivalent to a particle diameter of 5.2 nm. This is in close agreement with the TEM images. Particle size, crystallinity, and production rate can be controlled by varying the flow rates of H_2 and He to the reactor and by addition of SF_6. Changing these parameters allows us to produce particles with average diameters in the range of 5 to 20 nm. Larger particles are also easily produced, but are not presently of interest.

3.2 Photoluminescence induced by etching non-luminescent particles

Upon initial synthesis in the laser-driven reactor, the silicon nanoparticles exhibit little or no visible photoluminescence (PL) either as a dry powder or dispersed in solvents, although some weak PL in the infrared (beyond 850 nm) cannot be ruled out. After etching with HF/HNO_3 mixtures as described above, the particles exhibit bright visible PL. During the etching process, we believe that the nanoparticles are oxidized by HNO_3, and the resulting oxide is dissolved (etched) by HF, so that the size of the silicon core of the particles is reduced, and the surface is passivated with oxide produced by wet oxidation with HNO_3, rather than by the 'native oxide' that forms when the particles are exposed to room air. Powder samples and particle dispersions in water, methanol, and other solvents, with bright visible PL ranging from red to green have been produced. The emission wavelength decreases smoothly and monotonically with increasing etching time. This apparent size-dependent photoluminescence is comparable to that of the best published examples of silicon nanoparticles produced by electrochemical etching of silicon wafers[18]. Figure 2 shows the normalized PL spectra from a series of samples extracted at different times during etching of a single batch of nanoparticles. In this case, the peak PL emission wavelength decreases from near 855 nm to 570 nm with increasing etching time. In other samples, we have seen peaks in the PL spectrum at wavelengths below 500 nm after etching. For powder samples and particle dispersions with a peak PL wavelength near 600 nm, the photoluminescence intensity and spectrum is relatively stable. However, for dispersions of particles in water or methanol and for samples with initial peak PL emission at shorter wavelengths, the spectrum changes with time after the etching procedure. This is discussed further below.

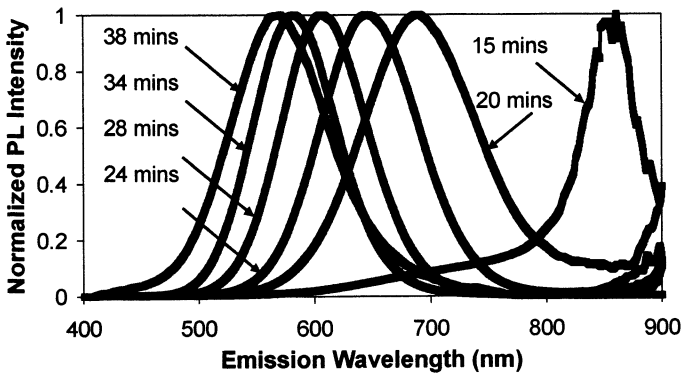

Figure 2: Normalized photoluminescence spectra of dry powder samples , showing the decrease in peak emission wavelength with increasing etching time (and presumably, therefore with decreasing particle size) in a roughly 3% HF/26% HNO_3 etching solution. The sensitivity of the R928 photomultiplier tube used here falls off sharply beyond 800 nm, and this is the source of the noisiness and odd shape of the 15 min spectrum. Spectra have been corrected for detector sensitivity and normalized.

3.3 Production of blue-emitting particles by rapid thermal oxidation (RTO)

We have not produced blue-emitting particles directly from the etching process described above, though it may yet prove possible to do so. However, we have produced blue emitting particle by rapid thermal oxidization (RTO) of particles that have peak emission in the orange before RTO. This was done by dispersing the etched particles in chloroform, which was then evaporated under dynamic vacuum with heating to 400 °C. Particles were then exposed to air for a short time (~1 minute), still at 400 °C. They were then cooled under dynamic vacuum. Figure 3 shows representative results of this rapid thermal oxidization procedure. For particles with original peak emission around 650 nm, after rapid thermal oxidization the peak emission shifted to 420 nm. The color change from orange to blue was accompanied by a slight increase in emission intensity. This process presumably causes the surface oxide layer on the particles to grow at the expense of the silicon core, decreasing the core size and shifting the emission wavelength toward the blue. However,

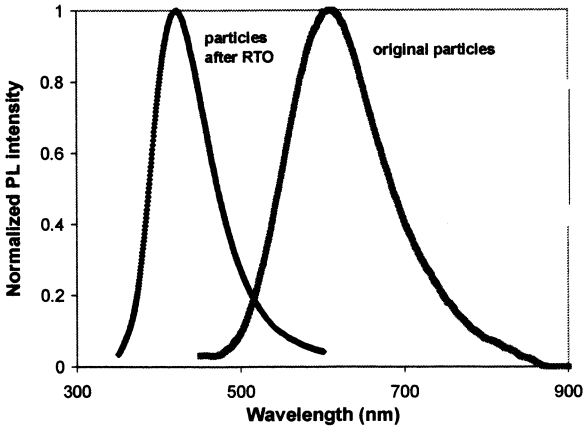

Figure 3: Normalized PL spectrum of blue-emitting nanoparticles and of the orange-emitting nanoparticles from which the blue-emitting particles were prepared. The inset shows chloroform dispersions of particles before and after rapid thermal oxidation, with UV illumination from below.

the mechanism of this emission is far from understood, and we do not claim that the change in emission wavelength is directly due to quantum confinement effects. In many cases, blue emission from Si particles is attributed to silicon sub-oxides, defects at the silicon/SiO_2 interface or other sources, and this may also be the case here. This emission is not present if the particles are oxidized completely (at higher temperature or for longer times) to yield SiO_2 nanoparticles. In any case, producing blue-emitting particles in this manner allows us to have PL emission spanning the entire visible spectrum, with comparable brightness for a range of wavelengths.

3.4 Stability of the silicon nanoparticle photoluminescence

A very important factor in the ultimate utility of these particles in applications and in investigations of their surface chemistry is the long-term stability of their optical properties. Lack of PL stability has significantly hampered applications of luminescent porous silicon. We have explored the stability of the PL from these particles, and their behavior is generally consistent with observations on porous Si. Figure 4 shows the time dependence of the PL spectrum of dispersions of silicon nanoparticles in methanol and water. For the methanol dispersion shown in figure 4a, the peak PL intensity dropped by a factor of 2.5 and the peak position shifted by about 12 nm toward the blue during the first 125 hours after etching. For water dispersions, the changes tend to be even larger. For the sample shown in figure 4b, the peak position shifted by almost 50 nm toward the blue and the intensity decreased by almost an order of magnitude during the first 31 hours after preparation. Most of the powder samples have shown no significant change in PL intensity or wavelength after several weeks of storage at room temperature in air, under fluorescent room lighting. The changes in PL intensity and emission wavelength may result from slow (ultimately self-limiting) oxidation of the particles, producing a thicker oxide layer and smaller core diameter, or may result from other changes in the state of the particle surface. The mechanism of luminescence in these particles is not yet firmly established, and therefore we can only speculate as to the source(s) of changes in it. We are investigating the stability of the PL further, and the surface treatment of the particles to stabilize their photoluminescence properties when dispersed in solvents. It should be emphasized that in the vast majority of samples, the changes in PL intensity described above have not led to a total loss of visible PL from the particles. We have many samples that, after 3 months of storage in air at room temperature exposed to room light, still show PL emission that is clearly visible to the unaided eye when excited by a 4-watt handheld UV lamp.

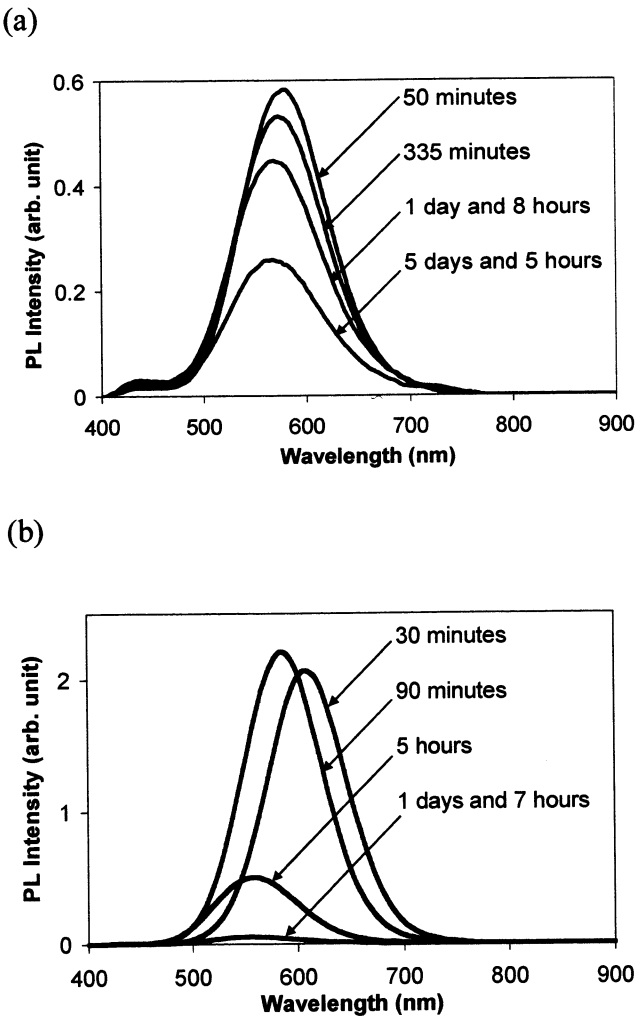

Figure 4: Change in PL emission spectrum with time after initial etching to produce luminescent particles. (a) particles dispersed in methanol, and (b) particles dispersed in water.

3.5 Stabilizing PL of silicon nanoparticles by wet oxidation

One means of stabilizing the PL from these nanoparticles is surface oxidization using HNO_3 or another oxidizer in solution. Chemical oxidization of Si nanoparticles may provide a high quality,

chemically inert, and relatively impermeable SiO_2 layer on the particle surface and therefore stabilize the emission by preventing further changes in the state of the particle surface. Figure 5 shows the PL from particles treated with 30% HNO_3 for 1.5 minutes immediately after etching, along with that from untreated particles. After about 13 days, the untreated particles in chloroform retained only about 6.5% of their initial emission intensity, while the particles oxidized with HNO_3 retained about 71% of their initial intensity. This is a vast improvement, but clearly not the complete, long-term stability that would be needed in some applications.

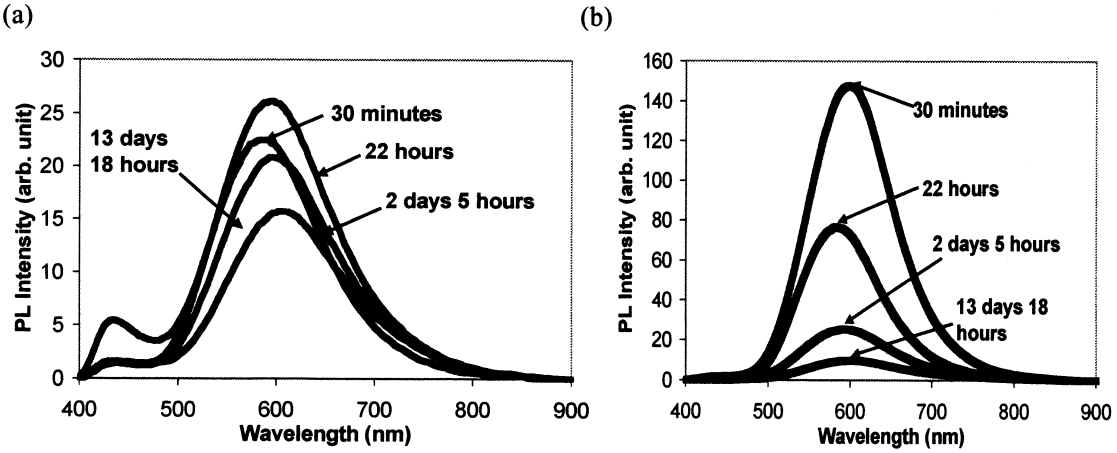

Figure 5: Time dependence of PL spectrum from silicon nanoparticles dispersed in chloroform after etching. The particles in (a) were washed for 1.5 minutes with 30% HNO_3 at the end of the etching procedure, while those in (b) were not. Note that the intensities cannot be compared directly between the two samples, due to differences in particle concentration, etc., but they can be compared quantitatively for the same sample at different times.

3.6 Stability of colloidal dispersions of silicon nanoparticles

In addition to lack of long-term stability, another concern for applications of these nanoparticles is their dispersability in a variety of solvents for processing, incorporation into polymeric hosts, dispersion in aqueous (biological) media, etc. While the particles produced here are easily dispersed into water, methanol, and other small alcohols by shaking or mild sonication, they agglomerate and partially settle out of these solvents over a period of several hours to several days at room temperature, and a period of minutes to a few hours at 80° C. By contrast, dispersions in 1,4-butanediol, 1,2-propanediol, and glycerol stay as stable colloidal dispersions for an extended period of time. These do not agglomerate overnight at 80° C or during several weeks of storage at room temperature. Work to modify the particles' surfaces not only to stabilize the PL, but also to make them more readily dispersable in a wider range of solvents is ongoing and preliminary results are described in the next section.

3.7 Preparation of stable colloidal dispersions of silicon nanoparticles

In order to make a truly thermodynamically stable dispersion of the etched Si nanoparticles, their surfaces must be adequately passivated. The hydrogen terminated Si particle surface is unstable, both toward slow oxidation by air and toward slow agglomeration in most solvents. Oxide-passivated surfaces are similarly unstable to agglomeration in most solvents and can suffer from further oxidation, which changes the photoluminescence spectrum. The approach described in recent work on surface alkylation by Lie et al.[33] has proven to be an effective method of rendering stability to the particles in nonpolar solvents like toluene. These authors have reacted different alkenes with the surface of luminescent silicon nanoparticles (produced by sonication of porous silicon) by refluxing the nanoparticles in toluene solutions of the alkenes. Such hydrosilylation reactions on porous silicon and on hydrogen terminated silicon wafers are well known, and are described in the review by Buriak[34]. Following similar procedures, powder samples and octadecene (approximately 1:1 weight ratio) were refluxed in toluene for 3-4 hours at 100 C under anaerobic conditions. This gave a yellowish but clear and fluorescent dispersion of Si particles in toluene that remained clear for several months. By using undecylenic acid instead of octadecene, it was possible to get a clear dispersion in a semi-polar solvent such as ethanol. With undecylenic acid bound to the surface, it was possible to

obtain an aqueous dispersion of the particles, but the clarity lasted only for a few days and eventually some turbidity developed.

The robust surface passivation thus rendered is understood by covalent chemical bonding of the ethylenic group of the alkene or alkenoic acid to the surface via a hydrosilylation reaction. This is evidenced by the FTIR spectra of the etched particles compared against the alkylated particles where a number of changes are notable. For these measurements, excess alkene or alkenoic acid was removed by dialysis after refluxing. The FTIR spectrum of the modified surface shows strong peaks characteristic of alkyl C-H_x vibration at 2923, 2852, 1657 and 1468 cm^{-1} that are not present in the untreated sample. The intensity of the Si-H feature (2108 cm^{-1}) decreases significantly in the treated sample. Comparing the treated sample to neat octadecene, the C=C features (991, 908 cm^{-1}) disappear, while all other spectral features retained. This shows that the silicon particle surfaces have been coated covalently and Si-C bonds are formed (which should appear at ~1083 cm^{-1}, overlapping with features due to Si-O bonds that are inevitably present). Similar results are obtained for particles treated with undecylenic acid. Again, the Si-H and double bond features disappear in the spectrum of the coated particles, which is otherwise essentially the sum of the undecylenic acid and untreated particle spectra.

3.8 Stabilization of photoluminescence by alkylation

The photoluminescence properties of the alkylated samples are greatly stabilized against degradation. Figure 6 shows the stability of the PL spectrum of a sample that had been treated with octadecene as described above. It was stored in air for 25 days with almost no change in PL intensity and no shift in PL peak position, while the PL spectrum of an untreated portion of the same sample decreased in intensity by a factor of about five and blue-shifted substantially. Both samples were stored in toluene under identical conditions. The PL of samples treated with undecylenic acid is also stabilized somewhat, but not to the same extent as for octadecene-treated particles. This could reflect a difference in the quality of the coating produced in the two cases, and improved undecylenic acid coatings may eventually provide the same long-term stabilization as octadecene coatings.

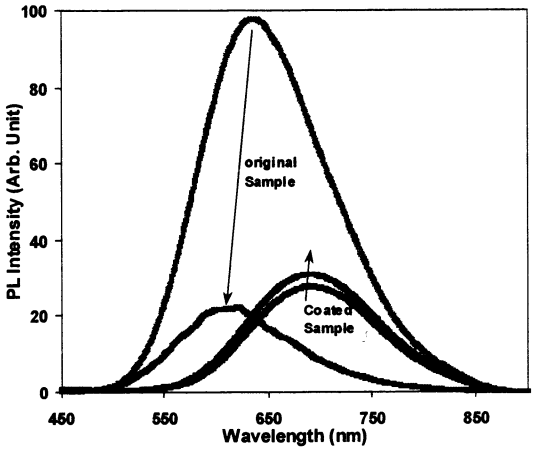

Figure 6: Stability of PL spectra of treated (alkylated) and untreated samples. Arrows point from before to after storage. The slight increase in PL intensity for the treated sample is probably due to a small amount of solvent (toluene) evaporation during the 25 days of storage.

3.9 Quenching of photoluminescence by Lewis bases:

In spite of the strong surface passivation by covalent bonding of organic species to the surface, the Si particle surfaces remain susceptible to quenching of photoluminescence by other species in solution. Quenching of PL in the case of porous silicon has been well investigated in the past and has been understood in terms of the polar attacking species providing a non-radiative recombination pathway for excitons[35]. It has been found that quenching induced by Lewis base amines is a reversible phenomenon and is pH dependent. This has been interpreted by a proton gated mechanism[36]. To explore this effect for the surface passivated nanoparticles prepared here, the transparent dispersion of Si particles was treated with different amines- primary, secondary and tertiary. Results are summarized here, and a fuller description will be published elsewhere. It was found that all the amines quench the PL, but with different efficiencies. In these experiments, the clear, stable, and homogeneous dispersion in ethanol of Si nanoparticles treated with undecylenic acid as discussed above was used. The PL of the neat sample showed a broad peak at about 650 nm. Identical volumes of 2M solutions in ethanol of primary, secondary and tertiary amine – namely ethylamine (EA), diethylamine (DA) and triethylamine (TA) - were added to identical fractions of the Si nanoparticle dispersion. The PL is essentially fully quenched by sufficient quantities of any of these amines. In order to determine the pH dependence and whether quenching by amines was a reversible effect, fixed aliquots of trifluoroacetic acid (TFA)

were added to each mixture. It was observed that the mixture containing triethylamine showed the maximum recovery of PL after excess TFA addition, and the mixture containing ethylamine.

It appears that the mechanism of quenching follows complex kinetics with a combination of steric factors, molecular dipole moment, and basicity of the amines possibly playing a role in quenching and recovery. We note that the original PL is never completely recovered, in spite of adding excess TFA in all cases (and accounting for sample dilution). Also, the recovery is not instantaneous. Reversing the order of addition of TFA and amines does not change the final PL spectrum, but up to 24 hours is required to achieve this final spectrum. The time evolution of the PL spectrum depends strongly on the order of addition of the TFA and amines. Steric hindrance, though inconsequential in determining the diffusion of amines onto the particles surface because of the dilute and clear dispersion employed in our study, could still play a role if the mechanism involves the amines forming a physically adsorbed layer on the surface. The bulkier tertiary amine would do so less efficiently than the smaller ones and therefore the tertiary TA would have the least quenching power. Also, among the three amines used in this study, TA has the smallest dipole moment, 0.66 D, as compared to EA (1.22 D) and DA (0.92 D). The variation of quenching efficiency on polarity is consistent with earlier studies on many molecular fluorophore systems and also on PSi, where it has been shown that quenching efficiency rises with the polarity of the solvent. As for the recovery of PL by addition of TFA, it is likely that protonation of the nitrogen lone electron pair can disengage the amine dipoles from the surface of Si particles. Because of higher basicity of TA (pK_a = 11.01), the protonation is easier than in EA (pKa = 10.807) or DA (pK_a = 10.489) and thereby the PL recovery is more pronounced.

3.10 Incorporation of silicon nanoparticles into host matrices

A variety of applications in the fields of chemical sensing and optoelectronics involve light-emitting species embedded within a transparent solid host. For example, a dye with chemically sensitive photoluminescence can be incorporated into a xerogel structure and used to sense analytes that change the intensity, lifetime, and/or spectrum of the dye luminescence. However, the toxicity and instability of such dyes often limit their applicability. The use of luminescent silicon nanoparticles in place of these dyes would overcome these limitations. Preliminary experiments have shown that the silicon nanoparticles described here can be embedded in both polymeric and xerogel matrices. They have been incorporated to two different matrices- namely polymethylmethacrylate (PMMA) and tetraethylorthosilicate (TEOS) gel. In the former, a chloroform dispersion of the particles is mixed with concentrated solution of PMMA in the same solvent. The reasonably viscous solution is drop cast or spin cast onto a clean glass or quartz slide. The particles are found to be well sequestered in a polymer matrix. Solid state Si^{29} NMR of the particles in the matrix gives a broad peak indicating the presence of particles in the matrix. In the other case an ethanolic dispersion of the particles is homogeneously mixed with TEOS and vigorously stirred in the presence of mineral acid such as HCl. After a few hours, a viscous sol is obtained which converts into a gel over several weeks of slow evaporation. It should be noted here that acidic hydrolysis of TEOS is preferred as the basic hydrolysis is associated with PL quenching similar to that found with Lewis bases described above. Figure 7 shows that the incorporation of

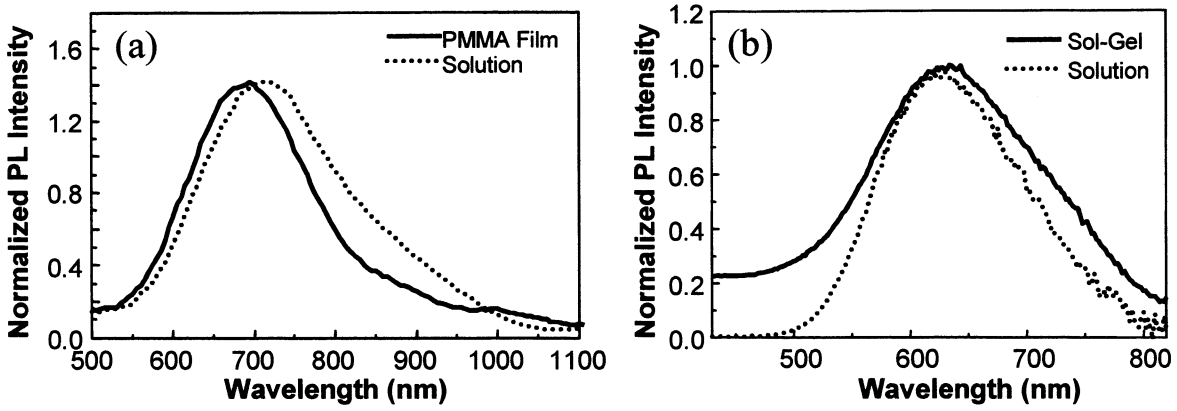

Figure 7. (a) PL from a set of Si nanoparticles in a PMMA film and in solution. (b) PL from a second set of nanoparticles in a sol-gel matrix and in solution. The short-wavelength emission from the sol-gel composite is due to the glass.

the nanoparticles into a poly(methylmethacrylate) (PMMA) film or into a xerogel structure has little effect on their photoluminescence spectra.

Recently, semiconductor nanoparticles have been utilized along with charge-conducting polymers to create quantum dot light emitting devices (QD-LEDs). The fabrication of these devices relies on the relatively simple techniques commonly utilized to produce organic LEDs. To date, the bulk of work in visible QD-LEDs has been concentrated on CdSe-based materials[37,38]. Silicon nanoparticles are strong candidates for use in these types of devices due to the wide range of wavelengths at which efficient luminescence can be obtained. However, initial studies have shown that electrically conducting polymers useful in constructing these devices, such as poly(9-vinylcarbazole), quench the silicon photoluminescence in a manner similar to the amines discussed in the previous section. In order to overcome these challenges, proper silicon-polymer systems must be selected and the silicon/polymer interfaces must be optimized such that charge carriers can be injected into the nanoparticles and preferentially recombine there rather than by non-radiative routes in the polymer or at the interface.

4. SUMMARY AND CONCLUSIONS

This paper summarizes our recent work on the preparation and functionalization of brightly luminescent silicon nanoparticles for applications in nanophotonics and biophotonics. Silicon nanoparticles with bright visible photoluminescence, spanning the entire visible spectrum, have been prepared by a new combined vapor-phase and solution-phase process, using only inexpensive commodity chemicals. Functionalizing the surface of these particles with organic molecules allows them to be well-dispersed in a variety of non-polar and semi-polar solvents. This surface functionalization also dramatically stabilizes the photoluminescence against degradation that occurs over a period of hours to weeks in untreated samples. However, it appears that even the functionalized particles are susceptible to chemical quenching of the photoluminescence by Lewis bases, particularly amines. This may be a challenge for preparation of light emitting devices, but could be an advantage in sensing applications. Preliminary experiments on the incorporation of these luminescent nanoparticles into both PMMA and sol-gel glass matrices have shown that the nanoparticles can be dispersed in these matrices and that their photoluminescence is little effected. However, the photoluminescence of particles dispersed in poly(9-vinylcarbazole) was quenched. Optimization of the conducting polymer matrix and its interface with the silicon nanoparticles will be required for production of light emitting devices based on silicon nanoparticle/polymer matrix nanocomposites. However, if such devices can be realized, they have enormous potential in applications ranging from solid-state lighting to flexible displays to chemical sensing.

5. ACKNOWLEDGEMENTS

This work was partially supported by the Defense University Research Initiative on Nanotechnology through AFOSR (Grant #F496200110358), an Integrative Graduate Education and Research Traineeship from NSF (Grant #DGE-0114330), the division of Chemical and Transport Systems of NSF (Grant #CTS-0087315), and the University at Buffalo (SUNY).

6. REFERENCES CITED

1 W. C. W. Chan and S. Nie, *Science* **281,** 2016-2018 (1998).
2. M. Bruchez, Jr., M. Moronne, P. Gin, S. Weiss, and A. P. Alivisatos, *Science* **281,** 2013-2015 (1998).
3. T. D. Lacoste, X. Michalet, F. Pinaud, D. Chemla, A. P. Alivisatos, and S. Weiss, *Proc. Natl. Acad. Sci.* **97,** 9461-9466 (2000).
4. D. J. Lockwood (Ed.), *Light Emission in Silicon From Physics to Devices* (Academic Press, New York, 1998).
5. W. R. Cannon, S. C. Danforth, J. H. Flint, J. S. Haggerty, and R. A. Marra, *J. Am. Ceram. Soc.* **65,** 324-330 (1982).
6. W. R. Cannon, S. C. Danforth, J. S. Haggerty, and R. A. Marra, *J. Am. Ceram. Soc.* **65,** 330-335 (1982).
7. L. T. Canham, *Appl. Phys. Lett.* **57,** 1046-1048 (1990).
8. W. L. Wilson, P. J. Szajowski, and L. Brus, *Science* **262,** 1242-1244 (1993).
9. K. A. Littau, P. J. Szajowski, A. J. Muller, A. R. Kortan, and L. Brus, *J. Phys. Chem.* **97,** 1224-1230 (1993).

10. L. Brus, J. Phys. Chem. **98,** 3575-3581 (1994).
11. L. E. Brus, P. J. Szajowski, W. L. Wilson, T. D. Harris, S. Schuppler, and P. H. Citrin, *J. Am. Chem. Soc.* **117,** 2915-2922 (1995).
12. J. A. Carlisle, M. Dongol, I. N. Germanenko, Y. B. Pithawalla, and M. S. El-Shall, *Chem. Phys. Lett.* **326,** 335-340 (2000).
13. Z. F. Ding, B. M. Quinn, S. K. Haram, L. E. Pell, B. A. Korgel, and A. J. Bard, *Science* **296,** 1293-1297 (2002).
14. D. S. English, L. E. Pell, Z. H. Yu, P. F. Barbara, and B. A. Korgel, *Nano Letters* **2,** 681-685 (2002).
15. J. D. Holmes, K. J. Ziegler, R. C. Doty, L. E. Pell, K. P. Johnston, and B. A. Korgel, *J. Am. Chem. Soc.* **123,** 3743-3748 (2001).
16. M. H. Nayfeh, N. Barry, J. Therrien, O. Akcakir, E. Gratton, and G. Belomoin, *Appl. Phys. Lett.* **78,** 1131-1133 (2001).
17. M. H. Nayfeh, O. Akcakir, G. Belomoin, N. Barry, J. Therrien, and E. Gratton, *Appl. Phys. Lett.* **77,** 4086-4088 (2000).
18. G. Belomoin, J. Therrien, A. Smith, S. Rao, R. Twesten, S. Chaieb, M. H. Nayfeh, L. Wagner, and L. Mitas, *Appl. Phys. Lett.* **80,** 841-843 (2002).
19. J. R. Heath, *Science* **258,** 1131-1133 (1992).
20. R. K. Baldwin, K. A. Pettigrew, E. Ratai, M. P. Augustine, and S. M. Kauzlarich, *Chem. Commun.* **17,** 1822-1823 (2002).
21. R. A. Bley and S. M. Kauzlarich, *J. Am. Chem. Soc.* **118,** 12461-12462 (1996).
22. Q. Liu and S. M. Kauzlarich, *Mater. Sci. Eng. B* **B96,** 72-75 (2002).
23. D. Mayeri, B. L. Phillips, M. P. Augustine, and S. M. Kauzlarich, *Chem. Mater.* **13,** 765-770 (2001).
24. C. Lam, Y. F. Zhang, Y. H. Tang, C. S. Lee, I. Bello, and S. T. Lee, *J. Crystal Growth* **220,** 466-470 (2000).
25. E. Borsella, M. Falconieri, S. Botti, S. Martelli, F. Bignoli, L. Costa, S. Grandi, L. Sangaletti, B. Allieri, and L. Depero, *Mater. Sci. Eng. B* **B79,** 55-62 (2001).
26. E. Borsella, S. Botti, M. Cremona, S. Martelli, R. M. Montereali, and A. Nesterenko, *J. Mater. Sci. Lett.* **16,** 221-223 (1997).
27. S. Botti, R. Coppola, F. Gourbilleau, and R. Rizk, *J. Appl. Phys.* **88,** 3396-3401 (2000).
28. M. Ehbrecht, B. Kohn, F. Huisken, M. A. Laguna, and V. Paillard, *Phys. Rev. B* **56,** 6958-6964 (1997).
29. F. Huisken and B. Kohn, *Appl. Phys. Lett.* **74,** 3776 (1999).
30. G. Ledoux, D. Amans, J. Gong, F. Huisken, F. Cichos, and J. Martin, *Mater. Sci. Eng.* **C 19,** 215-218 (2002).
31. G. Ledoux, J. Gong, F. Huisken, O. Guillois, and C. Reynaud, *Appl. Phys. Lett.* **80,** 4834-4836 (2002).
32. A. A. Seraphin, E. Werwa, and K. D. Kolenbrander, *J. Mater. Res.* **12,** 3386-3392 (1997).
33. L. H. Lie, M. Deuerdin, E. M. Tuite, A. Houlton, and B. R. Horrocks, *J. Electroanalytical Chem.* **538-539,** 183-190 (2002).
34. J. M. Buriak, *Chem. Rev.* **102,** 1271-1308 (2002).
35. J. M. Lauerhaas and M. J. Sailor, *Science* **261,** 1567-1568 (1993).
36. J. M. Lauerhaas, G. M. Credo, J. L. Heinrich, and M. J. Sailor, *J. Am. Chem. Soc.* **114,** 1911-1912 (1992).
37. V. L. Colvin, M. C. Schlamp, and A. P. Alivisatos, *Nature* **370,** 354-357 (1994).
38. S. Coe, W. K. Woo, M. G. Bawendi, and V. Bulovic, *Nature* **420,** 800-803 (2002).